ORIGINAL RESEARCH

Small-Airway Dysfunction is Involved in the Pathogenesis of Asthma: Evidence from Two Mouse Models

Yishu Xue*
Wuping Bao*
Yan Zhou*
Qiang Fu
Huijuan Hao
Lei Han
Dongning Yin
Yingying Zhang
Xue Zhang
Min Zhang

Department of Respiratory and Critical Care Medicine, Shanghai General Hospital, Shanghai Jiao Tong University School of Medicine, Shanghai, 200080, People's Republic of China

*These authors contributed equally to this work

Background: There has been growing evidence of small-airway dysfunction in patients with asthma. Few studies have evaluated the mechanism of small-airway dysfunction in mouse models of asthma.

Purpose: We explored the correlation between small-airway spirometric variables and large-airway function or inflammation in different endotypes of asthma.

Methods: Ovalbumin (OVA) sensitization/challenge was used to produce a type 2 (T2)-high asthma model, and OVA combined with ozone exposure (OVA + ozone) was used for the T2-low asthma model with increased neutrophils. Spirometry, airway responsiveness, cytokine levels in bronchoalveolar lavage fluid (BALF), and pathological analyses of lung slices stained with hematoxylin-eosin, periodic acid–Schiff, and Masson's trichrome stain were all determined. *Muc5ac* expression in lung tissue was evaluated by the reverse transcription-polymerase chain reaction (RT-PCR), and alpha-smooth muscle actin was measured by immunohistochemistry.

Results: Inflammatory cells infiltrated the lung tissue and inflammatory cytokines were increased in the BALF of both the OVA and OVA + ozone groups, compared with the control group. Peribronchial hypersecretion and collagen deposition were evident in the models. The OVA + ozone group showed greater neutrophilic infiltration and peribronchial smooth muscle proliferation than the OVA group. Large-airway obstruction, small-airway dysfunction, and airway hyperresponsiveness were confirmed in both models. Small-airway functional variables, such as MMEF (mean midexpiratory flow, average flow from 25 to 75% forced vital capacity [FVC]) and FEF50 (forced expiratory flow at 50% of FVC), were positively correlated with large-airway function and had a stronger negative correlation with airway inflammation, mucus secretion, and responsiveness than large-airway function.

Conclusion: Small-airway dysfunction was evident in the two endotypes of asthma and was correlated with severe airway inflammation, mucus hypersecretion, and airway hyperresponsiveness. The small airways may be an important target in asthma treatment, and further research in the role of small-airway variables in the pathogenesis of asthma is warranted.

Keywords: small airway, spirometry, airway inflammation, asthma, airway hyperresponsiveness

Correspondence: Min Zhang
Department of Respiratory and Critical Care Medicine, Shanghai General Hospital, Shanghai Jiao Tong University School of Medicine, No. 100, Haining Road, Shanghai, 200080, People's Republic of China
Email maggie_zhangmin@163.com

Introduction

Bronchial asthma was traditionally considered to affect mainly the large airways. However, increasing evidence shows that small-airway dysfunction, an overlooked respiratory abnormality, also contributes to the clinical features of asthma. The small airways in humans are bronchial passages less than 2 mm in diameter, located

beyond the seventh or eighth generation of the tracheo-bronchial tree. These airways terminate with the alveolar sacs and account for more than 98% of the cross-sectional area of the lung.[1]

The small airways play an important role in pathophysiologic mechanisms and the clinical manifestations of asthma. The typical chronic inflammation in asthma affects all airways, from the large proximal to the small distal airways. This has been proven in studies of lung biopsies from individuals with fatal asthma and surgical lung specimens from patients with chronic asthma.[2,3] A prospective cohort study showed that small-airway disease is present across different degrees of severity of asthma, but was especially common in severe asthma.[4] Moreover, a systematic review indicated that small-airway disease is pervasive in adult asthma, even in patients with mild disease.[5] However, there have been few studies on mouse models, with a focus on the role of small-airway dysfunction in the pathogenesis of asthma.

Small-airway abnormalities in humans could be evaluated by radiological and other noninvasive variables, such as airway wall thickness determined by high-resolution computed tomography, alveolar nitric oxide concentration, the difference in resistance from 5 to 20 Hz (R5–R20) in impulse oscillometry, and the late-phase eosinophil count in induced sputum.[6] The earliest change associated with airflow obstruction in the small airways is thought to be a slowing in the terminal section of the spirogram.[7] Therefore, variables from spirometry, such as the FEF50 (forced expiratory flow at 50% of forced vital capacity [FVC]), FEF75, and MMEF (mean midexpiratory flow, average flow between 25–75% FVC) are recommended to predict small-airway dysfunction in humans.[4] However, the analysis of the small airways in humans cited above cannot be completely duplicated in the mouse.

To evaluate lung function in mice, some studies of the large airways have been conducted through evaluation of the FEV0.1 (volume expired in the first 0.1 s of fast expiration) and FEV25 (volume expired in the first 25 ms of fast expiration)[8,9] using various test systems, similar to studies of the FEV1 (volume expired in the first 1 s of fast expiration) in humans. However, little attention has been given to the evaluation of small-airway function in an animal model of asthma. Using the EMMS eDacq Forced Manoeuvres system, large- and small-airway lung function tests were performed in mice, similar to those performed in human patients. The expiration portion of the flow-volume curve (see typical image in Figure S1 of

Supplementary information) displayed by the selected system for mice resembles that of humans.[10]

We designed mouse models of two endotypes, including the ovalbumin (OVA) sensitization/challenge–induced type 2 (T2)-high asthma model and the OVA combined with ozone exposure (OVA + ozone)–induced asthma model[11,12] with increased neutrophils, similar to T2-low asthma. We investigated the correlation between small-airway dysfunction and large-airway abnormality, as well as their relationship with airway inflammation and airway hyperresponsiveness in these mouse models. The important role and potential mechanism of small-airway dysfunction in the pathogenesis of asthma in mouse models were determined.

Materials and Methods
Animals
C57BL/6 mice (pathogen-free, male, age 5–6 weeks) were purchased from the SLRC Laboratory (Shanghai, China), and housed in controlled conditions of temperature (21–25 °C) and humidity (40–60%), with ad libitum access to water and food (free from OVA). Mice were acclimatized for 1 week before beginning the experiments with a 12-h light-dark cycle.

Allergic Airway Inflammation Induction and Ozone Exposure
C57BL/6 mice were randomly divided into three groups with eight mice in each group (see schematic diagram of mouse experiment in Figure S2 of Supplementary information). The OVA sensitization was administered on days 0 and 7, with an intraperitoneal (IP) injection of 20 μg OVA (Grade V, Sigma-Aldrich, St. Louis, MO) dissolved in 0.2 mL of Dulbecco's phosphate buffered saline (PBS), emulsified in 2 mg aluminum hydroxide (Sigma-Aldrich) as an adjuvant. Challenge of OVA was induced on days 14, 16, 18, 20, and 22, with exposure to 5% aerosolized OVA (20 mL, Grade II, Sigma-Aldrich) in a plastic box that was linked to an ultrasonic nebulizer (Clenny2 Aerosol, Medel, S. Polo di Torrile, Italy) for 30 min. Mice in the control group were sensitized and challenged with the same volume (0.2 mL for sensitization and 20 mL for challenge) of PBS as vehicle.

Mice were exposed to ozone at a concentration of 3 ppm, or air in a Perspex container 30 min after each OVA/PBS challenge on days 14, 16, 18, 20, and 22. Ozone was produced by an ozone generator (model 300 Ozoniser,

Aqua Medic, Germany). Every exposure lasted 2 h. Ozone concentration was continuously controlled and adjusted by an OS-4 ozone switch (Eco Sensors, KWJ Engineering Inc, California, USA). The control mice were exposed to air during this time.

Spirometry in Mice Using the Forced Manoeuvres System

Mice were anesthetized with Zoletil 50 (tiletamine hydrochloride and zolazepam hydrochloride, 25 mg/kg, Virbac S. A., France) and xylazine hydrochloride (10 mg/kg, Chang Sha Best Biological Technology Institute Co., Ltd, China) via IP injection, 24 h after the last challenge. Following tracheostomy, mice were fitted with a tracheal cannula, and attached to a plethysmograph with a pneumotachograph using the eSpira Forced Manoeuvres System for mice (EMMS, Hants, UK). The animal's lungs were inflated to a set tracheal pressure, and then exposed to a large negative pressure reservoir, forcing the mouse to exhale as quickly as possible, to mimic classical clinical spirometry. Variables, including the FVC, FEV25, FEV50, FEV75, FEF25 (forced expiratory flow at 25% of FVC), FEF50, FEF75, and MMEF, were calculated. Among them, the FEV25, FEV50, FEV75, and FEF25 represented large-airway function; whereas the FEF50, FEF75, and MMEF indicated small-airway function.

Airway Responsiveness

Anesthetized mice were ventilated (MiniVent, Hugo Sachs Electronik, Germany) at 180 breaths per min and a tidal volume of 210 μL in a whole-body plethysmograph with a pneumotachograph connected to a transducer (EMMS, Hants, UK), as previous described.[13] Lung resistance (R_L) was recorded during a 3-min period following the administration of increasing concentrations (4–256 mg/mL, 10 μL each time) of acetylcholine chloride (ACh, Sigma-Aldrich, USA). R_L was expressed as the percentage change from baseline R_L (measured following PBS nebulization). The ACh concentration required to elevate R_L by 100% from baseline was calculated (PC100). For convenience in the data analysis, values on the abscissa for the curve of R_L was converted to the logarithmic form. Thus, -log PC100 was considered an indication of airway hyperresponsiveness.[13]

Bronchoalveolar Lavage Collection and Measurements

After airway function tests were performed, mice were sacrificed. The trachea of each mouse was lavaged with three aliquots of 0.6 mL cold PBS through a polyethylene (PE-60) tube (0.72-mm inner diameter, 1.22-mm outer diameter). Bronchoalveolar lavage fluid (BALF) was retrieved[14] and the return volume was consistently ≥ 70% of the instilled volume. The BALF was then centrifuged at 3000 r/min for 10 min at 4 °C. Total cell counts were calculated by a hemocytometer under optical microscope. And the supernatant was used for the enzyme-linked immunosorbent assay (ELISA) using commercial kits (for IL-4, IL-5, IL-17A, TNF-α: ANOGEN, Ontario, Canada; for IL-13: Invitrogen, California, USA; and for IgE: Crystal Chem, United States), according to the manufacturer's protocol.

Analysis of Muc5ac Gene Expression

Muc5ac is a representative component of airway mucus. Total RNA was isolated from lung tissue using the TRIzol Reagent (Invitrogen). After the determination of concentration and purity, RNA was translated into cDNA using a cDNA reverse transcription kit (Applied Biosystems, CA, USA) in a PTC-200 Peltier Thermal Cycler (MJ Research, Watertown, MA, USA). Real-time quantitative PCR (RT-qPCR) was performed using a ViiA 7 Real-Time PCR System (Biosystems, CA, USA). The RT-PCR thermal cycling program was as follows: one cycle of pre-denaturation at 95 °C for 5 min; followed by 40 cycles of denaturation at 95 °C for 15 s; annealing at 60 °C for 30 s; and elongation at 72 °C for 30 s. Fluorescence intensity of the internal reference gene (β-actin) and target gene (*Muc5ac*) expression were detected. The relative expression of target genes was calculated by the $2^{-\Delta\Delta Ct}$ method.

The following primer sequences were used in the PCR:

β-actin: Forward-5′ CCT CTA TGC CAA CAC AGT 3′, Reverse-5′ AGC CAC CAA TCC ACA CAG 3′;

Muc5ac: Forward-5′ TCA CAT TTG ATG GCA CCT ACT 3′,

Reverse-5′ CAC ACG GAA GTA TCC AAA CAC 3′

Histological and Morphometric Analysis

After the lungs of mice were resected, the left lungs were inflated by injection of 4% paraformaldehyde to provide 20 cm of water pressure. They were then immersed overnight in paraformaldehyde, after which they were embedded in paraffin, and sectioned to expose the maximum surface area of lung tissue in the plane of the bronchial tree,[15] and prepared for subsequent staining. Morphological changes of the lung and airway epithelium

were assessed following hematoxylin-eosin (HE), periodic acid–Schiff (PAS), and Masson's trichrome staining.

Peribronchiolar and perivascular inflammation was observed in the HE- stained lung slices and scored on a scale from 0 to 3, as previously described.[13] The total number of leukocytes, neutrophils, eosinophils, and lymphocytes along the lobar bronchi and segmental bronchi were determined in 10 randomly selected, nonoverlapping fields under a magnification of 400× from two separate lung sections per animal. Average width of observed area was 100μm. The airway inflammatory cells infiltration density (per 100 μm) was calculated as the ratio of cells to the whole length of bronchial wall counted.

For PAS-stained sections, blue/purple cells were considered PAS-positive. Masson's trichrome staining was conducted as described previously.[16,17] The paraffin sections of the left lung mentioned above were stained with Masson's trichrome stain to identify collagen deposition, following the standard manufacturer's protocol. The blue areas around the airways were identified as subepithelial collagen deposition.[18] The percentages of the PAS-positive areas and Masson-stained areas in relation to the total epithelial area were calculated (Image J software, MD, USA).

Infiltration of inflammatory cells, and evaluation of airway mucus hypersecretion and collagen deposition were performed double-blind by two investigators independently.

Immunohistochemical Analyses

Airway smooth muscle (ASM) mass and airway mucus secretion was observed using immunohistochemical staining, based on the presence of alpha-smooth muscle actin (α-SMA) and Muc5ac protein in lung tissue sections with the mouse α-SMA antibody (Proteintech, Wuhan, China) and mouse Muc5ac antibody (GTX11335, GeneTex, USA), as previously described.[16]

The area of α-SMA–positive and Muc5ac-positive expression around the airway epithelial cells in the respective images were independently analyzed in a double-blind fashion by two investigators, using the Image J software.

Statistical Analysis

Statistical analysis was conducted and graphs were constructed using the GraphPad PRISM, version 5.0 software (GraphPad, San Diego, CA). The Spearman correlation coefficient matrix was constructed and Spearman rank correlation tests were performed using the R version

3.6.1 (Innovative Solutions, St. Louis, MO, USA). Data were expressed as the mean ± standard deviation (SD), unless otherwise indicated. The Kruskal–Wallis ANOVA with Bonferroni's post hoc test (for equal variance) or Dunnett's T3 post hoc test (for unequal variance) were used to evaluate the differences in variance between multiple groups. A posttest Mann–Whitney analysis was conducted to evaluate the differences in variance between two groups. The correlation between different variables was determined using Spearman analysis; $r > 0.4$ or < -0.4 was considered indicative of strong correlations, and r values between -0.4 and 0.4 were considered indicative of weak correlations if $P < 0.05$.

$P < 0.05$ was considered statistically significant.

Results
Large- and Small-Airway Dysfunction in Both T2-High and T2-Low Asthma Models

One mouse in the OVA group died during anesthesia and tracheostomy; thus, no data was collected on lung function or airway responsiveness, and no further testing or dissection was performed on this animal.

The FVC value showed no statistical difference among the three groups (Figure 1A). The mice selected for the experiments were of the same age and strain. Therefore, large-airway function was assessed based on the FEV25, FEV50, FEV75, and FEF25 values. The FEV50 showed a decline in both the OVA and OVA + ozone–treated mice compared with the control group (Figure 1C); whereas the OVA group alone seemed to have more considerable large-airway obstruction based on the decline in FEV25 values. However, FEV25 values in the OVA + ozone group exhibited no significant difference with the control group (Figure 1B). The FEV75 (Figure 1D) and FEF25 (Figure 1H) value showed no statistical difference among the three groups.

Small-airway dysfunction was evident in the different mouse models of asthma. The MMEF, FEF75, and FEF50 values all showed a decline in both the T2-high and T2-low mouse models of asthma compared with the control group (Figures 1E–G). Overall, small-airway dysfunction coexisted with large-airway dysfunction in both T2-high and T2-low asthma models and altered variables of the small airways were evident in both models.
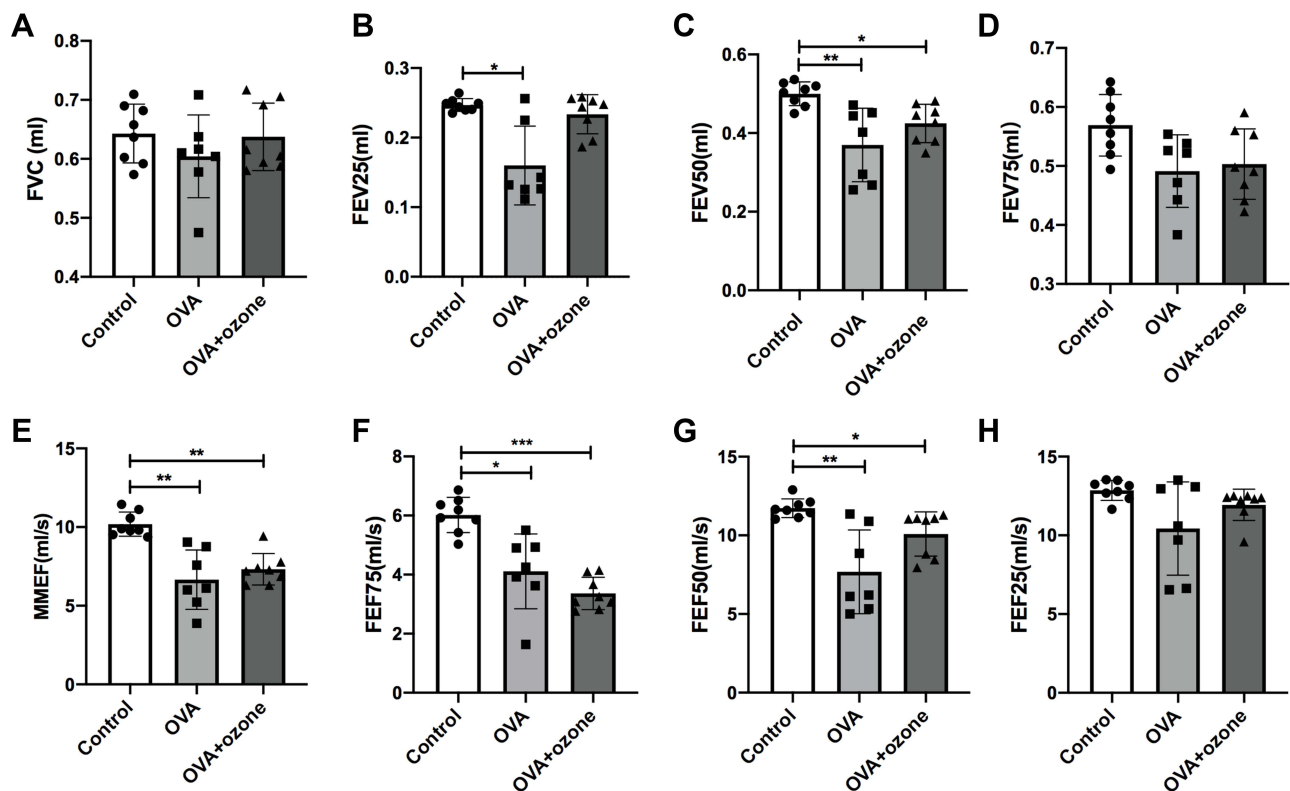
Figure 1 Large- and small-airway obstruction in mice representing different airway inflammation models. Airway function in mice was measured using a forced manoeuvres system. (**A**) FVC showed no difference between the control group and asthma models. (**B–D, H**) Large-airway function (FEV25, FEV50, FEV75, FEF25) in mice. (**E–G**) Small-airway function (FEF50, FEF75, MMEF) declined in mouse models of asthma. *P < 0.05, **P < 0.01, ***P < 0.001.
Abbreviations: FVC, forced vital capacity; FEF75, forced expiratory flow at 75% of FVC (25% expired); FEF50, forced expiratory flow at 50% of FVC; FEF25, forced expiratory flow at 25% of FVC (75% expired); FEV25, volume expired in the first 25 ms of fast expiration; FEV50, volume expired in the first 50 ms of fast expiration; FEV75, volume expired in first 75 ms of fast expiration; MMEF, mean mid expiratory flow, average flow from 25–75% FVC.

Mouse Models of Asthma Exhibited Airway Hyperresponsiveness

Following PBS nebulization, no significant differences in baseline R_L values were noted among the three groups (Figure 2A). After OVA sensitization/challenge, with or without ozone exposure, animals exhibited a leftward shift in the concentration responsiveness curve of R_L, suggesting an increased airway responsiveness compared with control mice (Figure 2C). In the control group, ACh caused a concentration-dependent increase in airway
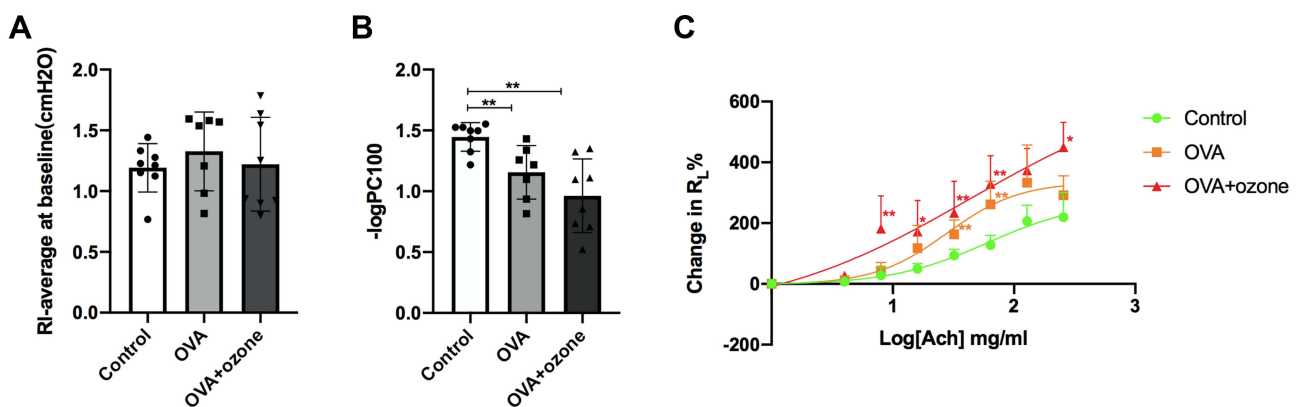

Figure 2 Asthma models exhibited bronchial hyperresponsiveness. (**A**) The baseline is represented by average lung resistance (R_L) value after PBS nebulization (within 2 min) for each mouse. (**B**) -logPC100 (ACh concentration required to increase R_L by 100% from baseline). (**C**) Mean percentage increase in R_L with increasing concentrations of ACh. Data are expressed as mean ± SD. In Panel B, **P < 0.01; in Panel C, *P < 0.05, **P < 0.01, compared with the control group.

resistance, where the maximum average R_L% (compared to baseline) value was 219.85%. The OVA sensitization/challenge increased R_L at the 32 and 64 mg/mL concentrations of ACh, compared with the control group.

The T2-low asthma model showed stronger airway responsiveness and significantly increased R_L values at the 8, 16, 32, 64, and 256 mg/mL concentrations of ACh, compared with the control group. Furthermore, -log PC100 declined after both OVA treatment and OVA combined with ozone exposure, compared with the control group (Figure 2B). These findings indicate that airway hyperresponsiveness existed in both mouse models of asthma.

OVA and OVA + Ozone Groups Presented Significant Airway Inflammation and Mucus Hypersecretion

Compared with the control group, peribronchial and perivascular infiltrations of mononuclear cells were observed in lung tissue in both asthma models, as well as bronchial wall thickening (Figure 3A). Inflammation scores indicated severe airway inflammation in the mouse models of asthma compared with the control group (Figure 3E). In both asthma models, eosinophilic infiltration around the airways was increased compared with the control group (Figure 3D). Mice exposed to ozone demonstrated greater neutrophilic infiltration than those exposed to OVA alone (Figure 3D). Total cell counts in BALF increased in both the OVA and the OVA + ozone group (Figure 3J). Total cell and neutrophils in BALF increased more in the OVA + ozone group, compared with that of the OVA group (Figures 3J–L). Eosinophils in BALF increased in both the OVA and the OVA + ozone group (Figure 3M).

Airway hypersecretion was observed in mice of both asthma models (Figure 3B). The PAS-positive area calculation demonstrated elevated mucus secretion in both the OVA group and the OVA + ozone group, compare with the control mice (Figure 3F). *Muc5ac* gene expression (Figure 3H) and Muc5ac-positive area (Figures 3C and G) were increased in lung of both the OVA and OVA + ozone groups, compared with the control group, which further indicated mucus hypersecretion in both T2-high asthma and T2-low asthma. In addition, the OVA + ozone group had more severe hypersecretion than the OVA group (a 42.84% increase in the PAS-positive areas around epithelial cells).

The levels of IgE in serum elevated in both the OVA and the OVA + ozone group (Figure 3I).

Increased Inflammatory Cytokine Levels in the BALF of Both Mouse Models of Asthma

Levels of the T2-related cytokines, IL-4, IL-5, and IL-13 were increased in both the OVA and OVA + ozone groups, compared with the control group (Figures 4A–C). Levels of IL-17A were significantly elevated in both asthma models; however, the OVA + ozone group exhibited higher levels of IL-17A than the OVA group (Figure 4D). Levels of TNF-α protein in the BALF showed no significant differences among the three groups (Figure 4E).

OVA Caused Peribronchial Collagen Deposition

OVA sensitization/challenge induced peribronchial collagen deposition (Figures 5A and B). Compared with the control group, collagen deposition was increased in both the OVA and OVA + ozone groups (the percentage increase over the control group were 137.00% and 104.52%, respectively), indicating airway remodeling in the asthma models. The T2-high model seemed to have shown more severe collagen deposition than the T2-low model; however, no significant differences were observed between the two models.

Airway Smooth Muscle Mass Was Increased in the OVA + Ozone Group

The ASM mass (indicated by stained α-SMA around the airway) was increased in lung slices from mice treated with OVA + ozone, compared with control mice by 75.48% (Figures 6A and B). The OVA group showed a slightly, but not significantly thicker ASM than the control group. The ASM mass in lung slices of the OVA + ozone mice was increased by 42.66% more than that of the OVA group (Figure 6B). Correlation analysis demonstrated that the α-SMA positive area was positively correlated with the FEV50 (Spearman r = 0.6014, P =0.0428), but no correlation with other large- or small-airway variables was observed (Figure S3 in Supplementary information).

Variables of Small-Airway Function Were Negatively Correlated with Inflammatory Cytokines in the BALF, Airway Responsiveness, and Mucus Secretion

Among all three groups, small-airway variables were positively correlated with large-airway function (Figure 7, P values of Figure 7 are shown in Table S1 of the
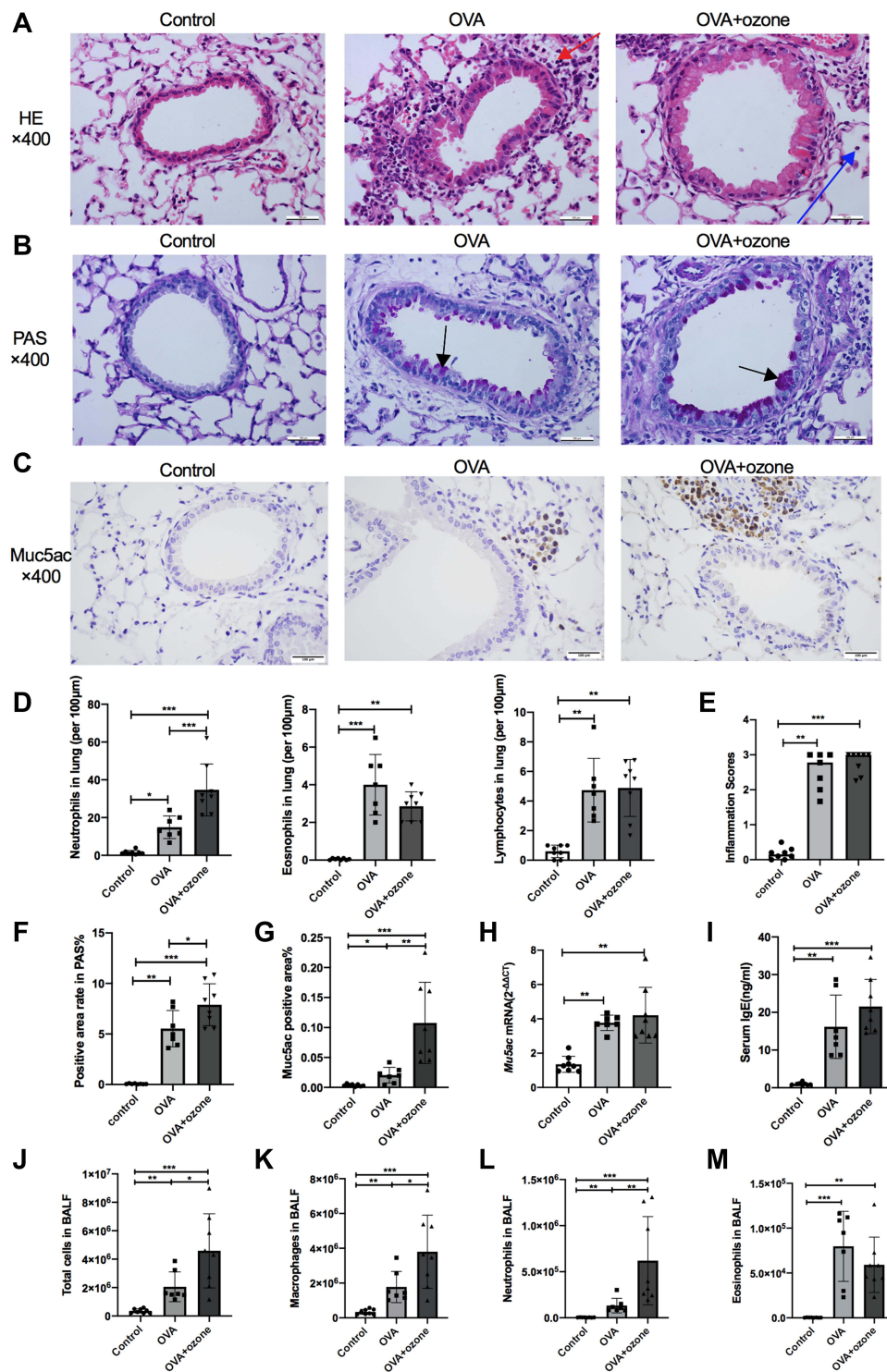
Figure 3 OVA and OVA + ozone–induced asthma models presented prominent airway inflammation and mucus hypersecretion. The infiltration of neutrophils, eosinophils, and lymphocytes, the PAS-positive area and Muc5ac-positive area were determined in a double-blind design by two investigators independently. *Muc5ac* mRNA in the lungs of mice was measured by RT-qPCR. (**A**) Representative photomicrographs of hematoxylin and eosin-stained sections of the lung with inflammatory cell infiltration (a typical neutrophil was indicated by a blue arrow and a typical eosinophil was indicated by a red arrow). (**B**) Representative photomicrographs of the lung with airway mucus production and goblet cell hyperplasia (purple area within tracheal cavity indicated by arrows). (**C**) Representative photomicrographs of immunohistochemical analysis of Muc5ac in lung tissue slices. (**D**) Infiltration density of neutrophils, eosinophils and lymphocytes. (**E**) Airway inflammation scores. (**F**) PAS-positive area. (**G**) Percentage of Muc5ac-positive area around the airways. (**H**) *Muc5ac* gene expression in lung tissue. (**I**) Levels of IgE in serum. (**J**) Total cells in BALF. (**K**) Macrophages in BALF. (**L**) Neutrophils in BALF. (**M**) Eosinophils in BALF. Scale bars represent 100 μm. Data in (**E**) are expressed as the median, as they did not fit a Gaussian distribution; other data are expressed as the mean ± SD. *P < 0.05, **P < 0.01, ***P < 0.001. Scale bars represent 100 μm.
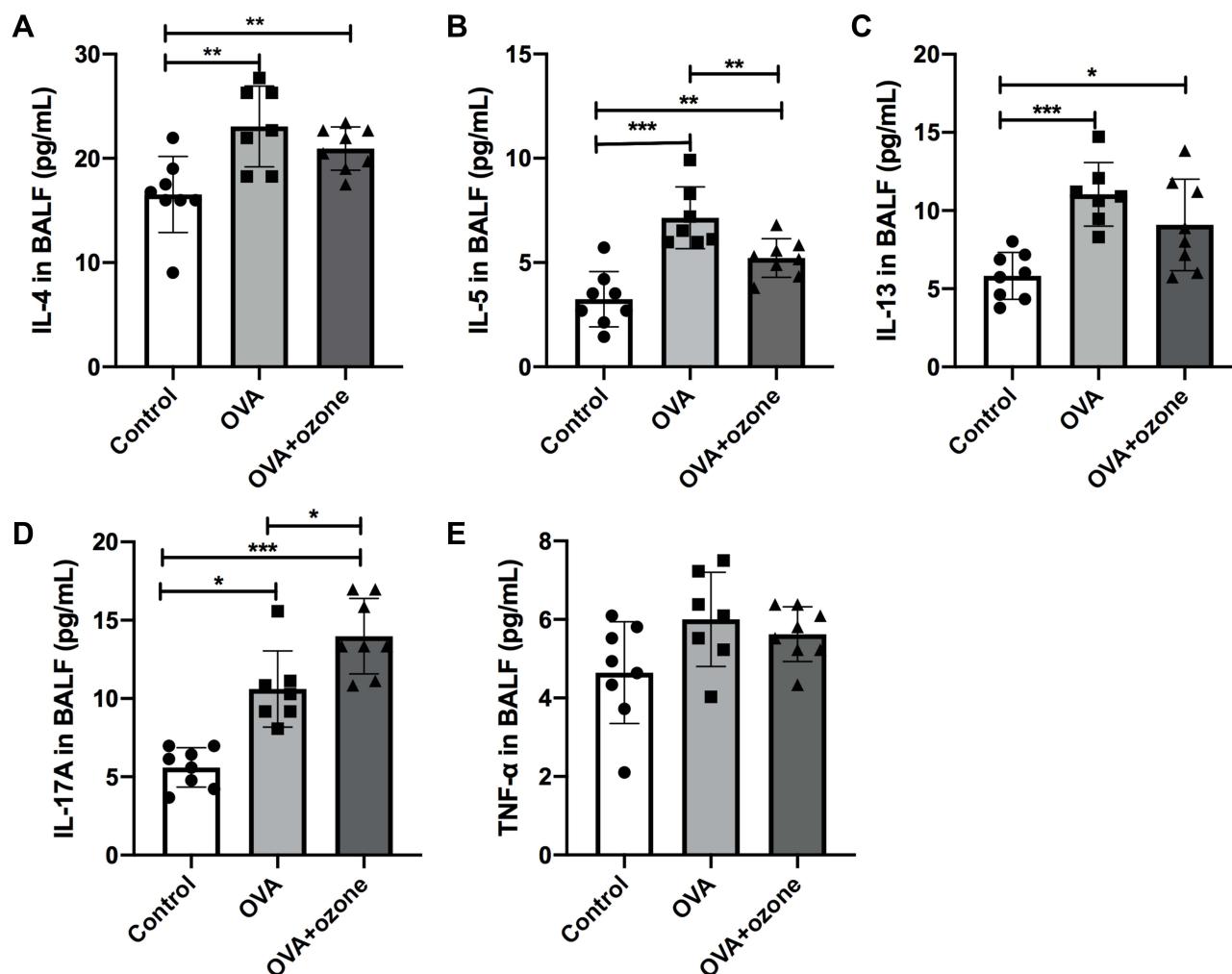**Abbreviation:** OVA, ovalbumin.

Figure 4 Levels of inflammatory cytokines in the bronchoalveolar lavage fluid (BALF) of asthmatic mouse models were increased. (**A**) Levels of IL-4 in BALF. (**B**) Levels of IL-5 in BALF. (**C**) Levels of IL-13 in BALF. (**D**) Levels of IL-17A in BALF. (**E**) Levels of TNF-α in BALF. *$P < 0.05$, **$P < 0.01$, ***$P < 0.001$.

Supplementary information). Furthermore, impaired airway function was accompanied by an aggravation of airway inflammation. Both small-airway and large-airway variables showed a negative correlation with the levels of inflammatory cytokines, such as IL-5, IL-13, and IL-17A in the BALF (Figure 7).

Large-airway variables, such as FEV50, were strongly and positively correlated with small-airway variables, especially with MMEF and FEF50 (The Spearman r being 0.61 and 0.68, respectively, and P value being 0.0018 and 0.0003 respectively). The MMEF and FEF50 demonstrated a positive correlation with both large-airway variables and small-airway variables.

The correlation between the respective indicators of large- and small-airway function, FEV50 and MMEF, and the levels of inflammatory cytokines in BALF were analyzed. The FEV50 and MMEF had a strong negative

correlation with levels of IL-5, IL-13, and IL-17A, indicating that both large- and small-airway function were related to airway inflammation. However, the indicators of small-airway function were more strongly correlated with these cytokines than those of large-airway function. Moreover, the MMEF, FEF50, and FEF75 all exhibited negative correlations with levels of IL-4, IL-5, IL-13, and IL-17A.

From another point of view, the levels of BALF cytokines showed a strong negative correlation with both large- and small-airway function, especially IL-5. Moreover, IL-13 and IL-17A showed stronger correlation with small-airway function than large-airway function. The Spearman r values between IL-13 levels and the MMEF and FEF50 were −0.65 (P= 0.0008) and −0.45 (P= 0.0307), respectively. A similar correlation was observed for IL-17A, as the Spearman r values for the
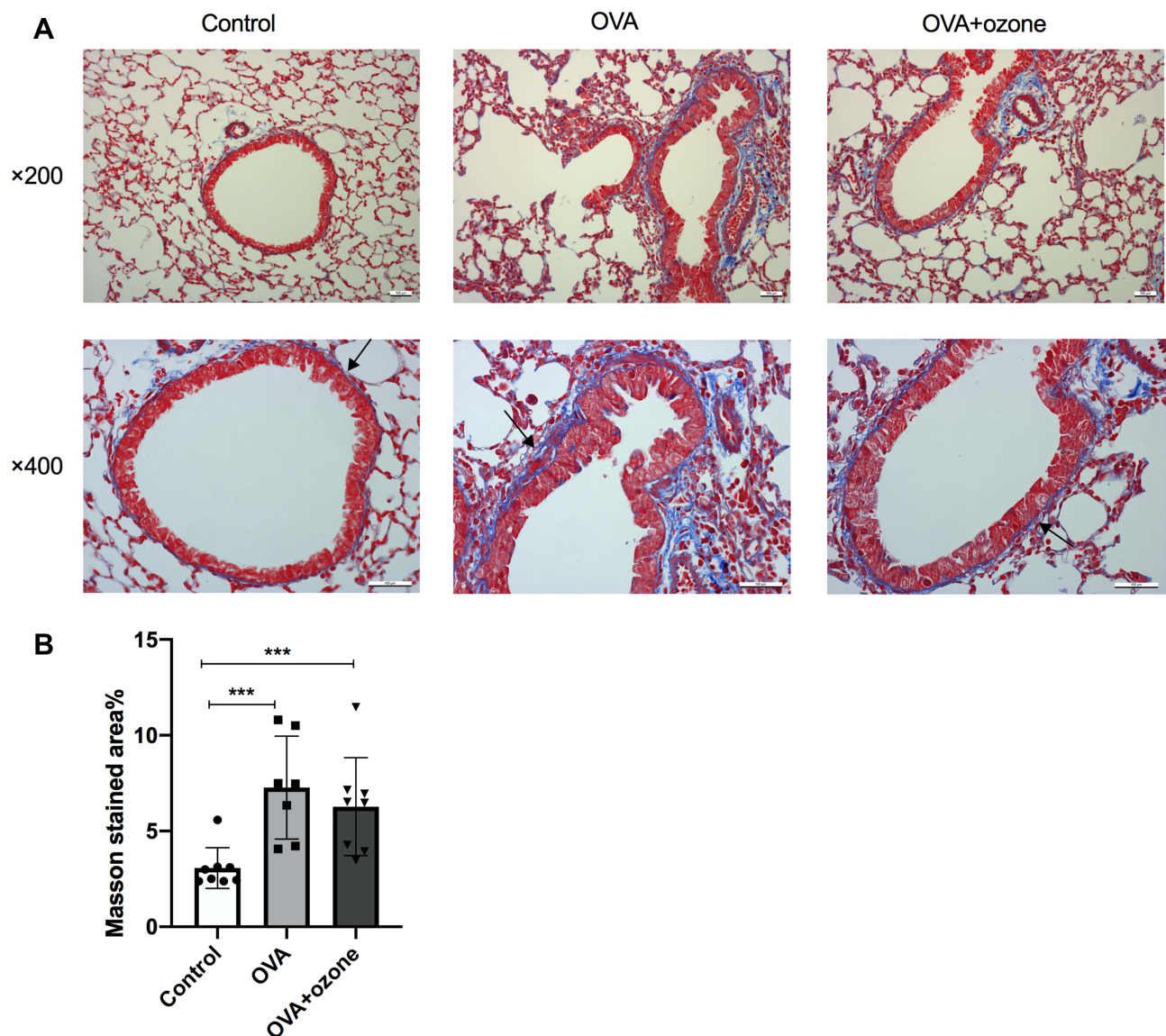
Figure 5 Collagen deposition in the lungs of mouse models of asthma. (**A**) Representative photomicrographs of Masson's trichrome stained lung tissue. (**B**) Percentage of subepithelial Masson stained area (blue area around airways were identified as collagen deposition and were indicated by arrows). ***P < 0.001. Scale bars represent 100 μm.

MMEF, FEF75, and FEF50 were −0.59 (P= 0.0032), −0.68 (P= 0.0419), and-0.43 (P= 0.0379), respectively.

Muc5ac gene expression in lung tissue was correlated with both large- and small-airway function indexes, and showed greater relevance for small-airway function. The Spearman r values between *Muc5ac* gene expression and the FEV50 and MMEF were −0.52 (P= 0.0043) and −0.74 (P= 0.0001), respectively.

As an indicator of airway responsiveness, -logPC100 was positively correlated with large- and small-airway function. Thus, small-airway function was negatively correlated with airway reactivity. A stronger correlation between -logPC100 and small-airway function was evident

(r = −0.44, P= 0.0378 for MMEF), compared with central airway variables. In addition, -logPC100 was negatively correlated with IL-4, IL-5, IL-13, and IL-17A protein levels in the BALF and *Muc5ac* gene expression in lung tissue.

Discussion

The two mouse models in the present study demonstrated asthma-like signs, such as airway inflammation, mucus hypersecretion, peribronchial collagen deposition, and airway hyperresponsiveness, compared with the control group. Mice treated with OVA showed severe eosinophilic inflammation as the T2-high asthma endotype. The OVA + ozone group demonstrated neutrophilic infiltration, similar
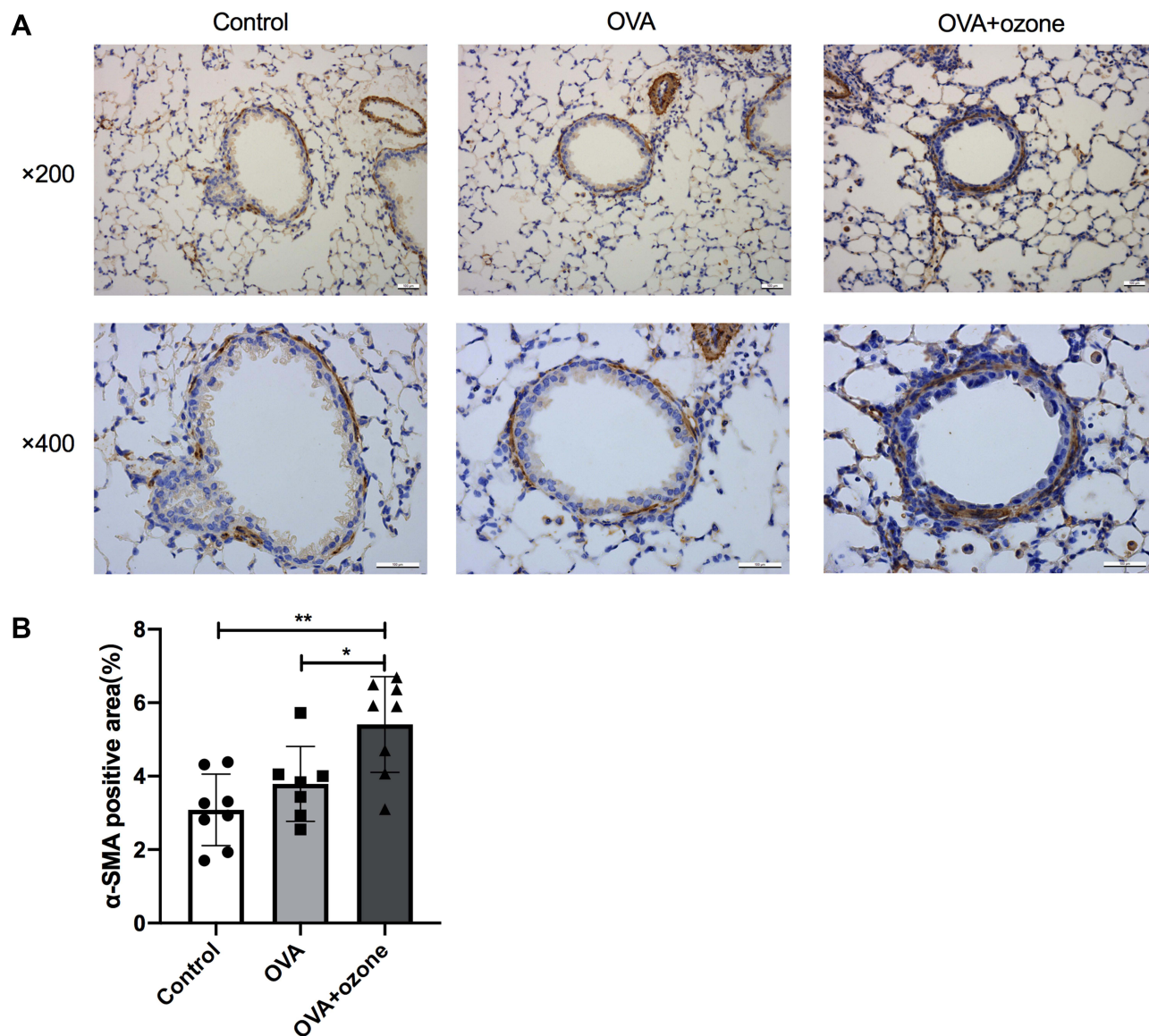
Figure 6 Airway smooth muscle (ASM) mass was increased in OVA + ozone mice. (**A**) Representative photomicrographs of immunohistochemical analysis of alpha-smooth muscle actin (α-SMA) in lung tissue slices. (**B**) Percentage of SMA-positive area around the airways. *P < 0.05, **P < 0.01. Scale bars represent 100 µm.

to that observed in our previous study, which may represent T2-low asthma.[13] Using these two models of asthma, we observed small-airway variables using spirometry and evaluated the correlations between small-airway variables and large-airway function, cytokines levels in the BALF, airway responsiveness, and *Muc5ac* gene expression. Our results demonstrated the role of small-airway dysfunction in the pathogenesis of asthma and provided a basis for subsequent animal studies on the pathogenesis and treatment of small-airway disease.

Ozone exposure has been shown to disrupt large-airway function in mice.[9,19,20] Similarly, we have shown that ozone exposure can induce a decline in FEV50.

Furthermore, in the present study, we emphasized the impairment of small-airway function in mouse models of asthma. The pathology of small-airway disease in mice has been investigated and defined diversely by different studies by determining the distance from the bronchioalveolar duct junction or the diameter of the airway ranging from < 100 µm to < 400 µm.[21–23]

To be more objective, we evaluated the change in the small airways according to functional variables. By using the EMMS eDacq Forced Manoeuvres system in mice, we showed that small-airway dysfunction exists in different endotypes of asthma. Clinical studies have shown that small-airway disease plays an important role in patients
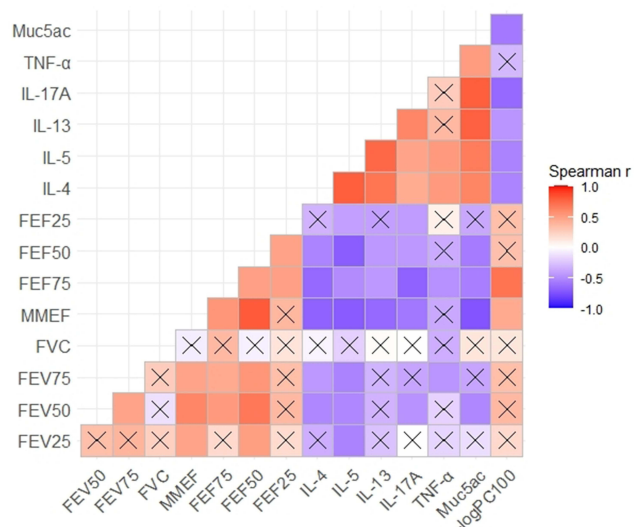
Figure 7 Small-airway function variables were negatively correlated with the levels of inflammatory cytokines in bronchoalveolar lavage fluid (BALF), airway responsiveness, and mucus secretion. A Spearman correlation coefficient matrix was constructed and Spearman rank correlation tests were conducted. A cross indicates no statistical significance.

with asthma.[4,5] Previous studies have assessed small-airway function using the precision-cut lung slice technique in vitro;[24] however, in the present study, small-airway responses were measured in vivo. Only a few studies have discussed small-airway function in mice.

The present study demonstrates that small-airway variables such as FEF50 and MMEF are correlated with the severity of airway inflammation, as indicated by IL-4, IL-5, IL-13 and IL-17A levels in the BALF. Similarly, several previous clinical studies have shown that small airways are thickened in asthma owing to chronic inflammation of the epithelium, submucosa, and muscle, with increased numbers of neutrophils, eosinophils, and lymphocytes, accompanied by increased mRNA expression of IL-4, IL-5.[3,25–27] Small-airway dysfunction may contribute to the progression of airway inflammation in asthma or could assist in evaluating the severity of the illness.

Among the cytokines related to airway inflammation, IL-13 and IL-17A showed greater correlation with small-airway function variables, such as FEF50, FEF75, and compared with large-airway variables. Furthermore, there was a strong correlation between IL-13 and IL-17A, and airway responsiveness, which may contribute to small-airway dysfunction. The possible relationship between IL-13 and the small airways in vitro has been previously discussed. Rat lung slices incubated with IL-13 in vitro induced higher small-airway sensitivity to carbachol and 5-hydroxytryptamine.[28] Similarly, treatment with IL-13,

but not IL-17A, in vitro increased the airway responsiveness of human bronchi (0.5–2.0 mm) induced by histamine, carbachol, or leukotriene D_4 in isolated human small airways.[29]

To our knowledge, no research has yet been conducted on the relationship between IL-17A and the small airways in asthma. We observed a correlation between IL-13 and IL-17A, and small-airway function in vivo, which further suggests that IL-13 and IL-17A are potential treatment targets for small-airway dysfunction in asthma. Regarding the asthma endotypes, we observed a significant increase in IL-17A levels in T2-low asthma in the present study. Furthermore, IL-17A mAb can alleviate airway inflammation and glucocorticoid insensitivity in a murine asthma model induced by OVA and ozone.[30] Therefore, IL-17A may contribute to, or interact with small-airway dysfunction in T2-low asthma.

Airway responsiveness showed a significant correlation with the severity of airway inflammation. In addition, airway responsiveness was correlated with small-airway function in the present models of asthma. Furthermore, MMEF combined with fractional exhaled nitric oxide (FENO) could credibly predict bronchial hyperresponsiveness (BHR) in clinical research,[31] suggesting the diagnostic value of evaluating small-airway function combined with airway inflammation for BHR. Our findings further prove previous discoveries in patients and further emphasize that small-airway function and airway inflammation are associated with airway hyperresponsiveness in the pathogenesis of asthma.

Interestingly, we found that airway responsiveness exhibited a stronger correlation with small-airway variables than large-airway variables, which could be attributed to the degree of airflow limitation in the small airways. The association between airway responsiveness and small-airway function has also been observed in previous clinical studies. Small-airway dysfunction was strongly associated with increased dyspnea during bronchial provocation with methacholine.[32] Similarly, children with atopic asthma have demonstrated a significant correlation between the PC20 (concentration of methacholine that induces a 20% decline in FEV1) and MMEF.[33] From a treatment perspective, extrafine-particle inhaled corticosteroids (ICS) improve airway hyperresponsiveness better than fine-particle ICS,[34] highlighting the importance of treatment reaching farther into the airways. Therefore, small-airway function should not be ignored in the diagnosis, treatment,

and prognosis of airway hyperresponsiveness in patients with asthma.

Mucus hypersecretion is another characteristic of asthma. The polymeric mucin, Muc5ac is an important component of airway mucus. *Muc5ac* gene expression is altered in asthma and contributes to its pathogenesis.[35] Higher expression of the *Muc5ac* gene and increased Muc5ac-positive area were observed in the lungs of T2-high and T2-low asthma models. Notably, *Muc5ac* gene expression was more strongly correlated with small-airway function than large-airway function.

Similarly, in humans, the mucosal surface area is relatively larger in the distal airways than the proximal airways (particularly after the eighth generation, which are smaller than 2 mm in diameter).[36] Thus, the surface area of the small airways may produce more mucus and contribute more to airway hypersecretion in the pathogenesis of asthma than that of the large airways, which help to explain our findings. Furthermore, the elevated expression of the *Muc5ac* gene in OVA + ozone mice suggests that such treatment reduces mucus secretion can be considered for patients with T2-low asthma.

Peribronchial collagen deposition and increased ASM are manifestations of airway remodeling.[37] The α-SMA is expressed by and used as a marker of smooth muscle cells.[38] We observed peribronchial collagen deposition in T2-high and T2-low asthma models. Furthermore, α-SMA levels were increased in lung tissue of the OVA + ozone group, which suggests an expansion of ASM mass in the T2-low asthma model. It has been widely acknowledged that chronic airway remodeling underlies the manifestations of asthma,[39] but whether and by how much ASM mass influences small-airway function in the early stages of airway inflammation is still unclear.[40]

Based on the present results, it may not necessarily be ASM mass alone, but other indicators such as airway inflammation and mucus hypersecretion, which affect small-airway function in our model of T2-high asthma with a short-term exposure that induces mild airway remodeling. Neutrophils may also play a part in promoting airway remodeling,[41] which may help explain the present results in the T2-low asthma model showing more severe airway remodeling than the T2-high model.

Furthermore, there may be different mechanisms of small-airway dysfunction in T2-high and T2-low asthma models, in spite of their approximate results in small-airway function. The OVA sensitization/challenge induced more Th2-related cytokines such as IL-5,

compared with OVA + ozone exposure; whereas the latter produced higher levels of IL-17A and demonstrated more severe neutrophilic infiltration within lung tissue. The OVA + ozone group showed increased ASM mass as well, which may also affect small-airway function. Therefore, treatment of the two types of asthma should be individualized and further studies of the potential signaling pathways involved in small-airway abnormality are warranted.

The effectiveness and practicality of variables mentioned above to evaluate small-airway function and its correlations with large-airway obstruction and inflammation, mucus secretion, and airway responsiveness deserve special consideration. Clinicians should identify the subpopulation of patients with asthma and small-airway disease, and attempt to improve the small-airway function in treatment. Further research on the mechanisms of small-airway dysfunction and the development of ultrafine-particle drugs may be needed.

Our findings provide relevant data for small-airway functional assessments and determination of the potential mechanisms in animal experiments. However, there are several limitations of the current study. First, there is a lack of experiments on the sequence of large airways and small airways in the pathogenesis of asthma. Further investigations would be conducted to determine whether small-airway dysfunction occurs before large-airway dysfunction or not. Next, the potential differences in mechanisms between small-airway dysfunction and large-airway dysfunction should be further investigated in the future.

Conclusion

Small-airway dysfunction is a feature of both T2-high and T2-low mouse models of asthma and is associated with airway inflammation, mucus hypersecretion, and airway hyperresponsiveness. Furthermore, in different endotypes of the asthma model, the mechanism of small-airway dysfunction may differ. Both IL-5 and IL-13 may play a greater role in small-airway dysfunction of T2-high asthma than T2-low asthma; whereas in T2-low asthma, IL-17A and increased ASM may be the more important factors. The small airways may be an important treatment target and should have a greater focus in future animal studies in asthma. It is important to establish fully evaluated mouse models of small-airway disease for further investigations of the underlying mechanisms and individualized treatment of asthma.

Abbreviations

α-SMA, α-smooth muscle actin; BALF, Bronchoalveolar lavage fluid; BHR, Bronchial hyperresponsiveness; ELISA, Enzyme-linked immunosorbent assay; FEV0.1, Volume expired in first 0.1s of fast expiration; FEV1, Volume expired in first 1s of fast expiration; FEF75, Forced Expiratory Flow at 75% of Forced Vital Capacity; FEF50, Forced Expiratory Flow at 50% of Forced Vital Capacity; FEF25, Forced Expiratory Flow at 25% of Forced Vital Capacity; FENO, Fractional exhaled nitric oxide; FEV25, Volume expired in first 25ms of fast expiration; FEV50, Volume expired in first 50ms of fast expiration; FEV75, Volume expired in first 75ms of fast expiration; FVC, Forced vital capacity; HE, Hematoxylin-Eosin; ICS, Inhaled corticosteroids; MMEF, Forced expiratory flow between 25 and 75% FVC; OVA, ovalbumin; PAS, Periodic Acid-Schiff; PC20, the concentration of methacholine that induces a 20% decline in FEV1; PC100, the ACh concentration demanded to elevate R_L by 100% from baseline was calculated; R5-R20, peripheral airway resistance as the difference between 5 and 20 Hz; R_L, lung resistance.

Study Approval and Ethics Statement

The study was approved by the Ethics Committee for Animal Studies at Shanghai General Hospital, China (IACUC: 2019-A011-01) and carried out in accordance with the Guide for the Care and Use of Laboratory Animals (National Academies Press, 2011). All surgeries were performed under anesthesia, and all efforts were made to minimize the suffering of animals. The experimental protocols were approved by Shanghai General Hospital Institutional Review Board, Shanghai, China.

Funding

Disclosure

The authors report no conflicts of interest in this work.

References

1. Carr TF, Altisheh R, Zitt M. Small airways disease and severe asthma. *World Allergy Organ J*. 2017;10(1):20. doi:10.1186/s40413-017-0153-4
2. Kuyper LM, Pare PD, Hogg JC, et al. Characterization of airway plugging in fatal asthma. *Am J Med*. 2003;115(1):6–11. doi:10.1016/S0002-9343(03)00241-9
3. Hamid Q, Song Y, Kotsimbos TC, et al. Inflammation of small airways in asthma. *J Allergy Clin Immunol*. 1997;100(1):44–51. doi:10.1016/S0091-6749(97)70193-3
4. Postma DS, Brightling C, Baldi S, et al. Exploring the relevance and extent of small airways dysfunction in asthma (ATLANTIS): baseline data from a prospective cohort study [published correction appears in Lancet Respir Med. 2019 Sep;7(9):e28]. *Lancet Respir Med*. 2019;7 (5):402–416. doi:10.1016/S2213-2600(19)30049-9
5. Usmani OS, Singh D, Spinola M, Bizzi A, Barnes PJ. The prevalence of small airways disease in adult asthma: a systematic literature review. *Respir Med*. 2016;116:19–27. doi:10.1016/j.rmed.2016.05. 006
6. Chen X, Wang K, Jiang M, et al. Leukotriene receptor antagonists for small-airway abnormalities in asthmatics: a systematic review and meta-analysis. *J Asthma*. 2013;50(7):695–704. doi:10.3109/02770 903.2013.806543
7. Pellegrino R, Viegi G, Brusasco V, et al. Interpretative strategies for lung function tests. *Eur Respir J*. 2005;26(5):948–968. doi:10.1183/ 09031936.05.00035205
8. Devos FC, Maaske A, Robichaud A, et al. Forced expiration measurements in mouse models of obstructive and restrictive lung diseases. *Respir Res*. 2017;18(1):123. doi:10.1186/s12931-017-0610-1
9. Fei X, Bao W, Zhang P, et al. Inhalation of progesterone inhibits chronic airway inflammation of mice exposed to ozone. *Mol Immunol*. 2017;85:174–184. doi:10.1016/j.molimm.2017.02.006
10. Heckman EJ, O'Connor GT. Pulmonary function tests for diagnosing lung disease. *JAMA*. 2015;313(22):2278–2279. doi:10.1001/jama.2015.4466
11. Last JA, Ward R, Temple L, et al. Ovalbumin-induced airway inflammation and fibrosis in mice also exposed to ozone. *Inhal Toxicol*. 2004;16(1):33–43. doi:10.1080/08958370490258237
12. Zhang JH, Yang X, Chen YP, et al. Nrf2 activator RTA-408 protects against ozone-induced acute asthma exacerbation by suppressing ROS and γδT17 Cells. *Inflammation*. 2019;42(5):1843–1856. doi:10. 1007/s10753-019-01046-6
13. Bao W, Zhang Y, Zhang M, et al. Effects of ozone repeated short exposures on the airway/lung inflammation, airway hyperresponsiveness and mucus production in a mouse model of ovalbumin-induced asthma. *Biomed Pharmacother*. 2018;101:293–303.14. doi:10.1016/j. biopha.2018.02.079
14. Li F, Zhang P, Zhang M, et al. Hydrogen sulfide prevents and partially reverses ozone-induced features of lung inflammation and emphysema in mice. *Am J Respir Cell Mol Biol*. 2016;55(1):72–81. doi:10.1165/rcmb.2015-0014OC
15. Pinart M, Hussain F, Shirali S, et al. Role of mitogen-activated protein kinase phosphatase-1 in corticosteroid insensitivity of chronic oxidant lung injury. *Eur J Pharmacol*. 2014;744:108–114. doi:10. 1016/j.ejphar.2014.10.003
16. Zhang X, Bao W, Fei X, et al. Progesterone attenuates airway remodeling and glucocorticoid resistance in a murine model of exposing to ozone. *Mol Immunol*. 2018;96:69–77. doi:10.1016/j. molimm.2018.02.009
17. Zhang L, Chi X, Luo W, et al. Lung myofibroblast transition and fibrosis is regulated by circ0044226. *Int J Biochem Cell Biol*. 2020;118:105660. doi:10.1016/j.biocel.2019.105660
18. Royce SG, Miao YR, Lee M, et al. Relaxin reverses airway remodeling and airway dysfunction in allergic airways disease. *Endocrinology*. 2009;150(6):2692–2699. doi:10.1210/en.2008-1457

19. Li F, Wiegman C, Seiffert JM, et al. Effects of N-acetylcysteine in ozone-induced chronic obstructive pulmonary disease model. *PLoS One*. 2013;8(11):e80782. doi:10.1371/journal.pone.0080782

20. Sun Z, Li F, Zhou X, Wang W. Generation of a chronic obstructive pulmonary disease model in mice by repeated ozone exposure. *J Vis Exp*. 2017;126:56095.

21. Liu JQ, Yang D, Folz RJ. A novel bronchial ring bioassay for the evaluation of small airway smooth muscle function in mice. *Am J Physiol Lung Cell Mol Physiol*. 2006;291(2):L281–L288. doi:10.1152/ajplung.00320.2005

22. Sera T, Uesugi K, Himeno R, Yagi N. Small airway changes in healthy and ovalbumin-treated mice during quasi-static lung inflation. *Respir Physiol Neurobiol*. 2007;156(3):304–311. doi:10.1016/j.resp.2006.11.006

23. Uemasu K, Tanabe N, Tanimura K, et al. Serine protease imbalance in the small airways and development of centrilobular emphysema in chronic obstructive pulmonary disease. *Am J Respir Cell Mol Biol*. 2020;63(1):67–78. doi:10.1165/rcmb.2019-0377OC

24. Donovan C, Royce SG, Esposito J, et al. Differential effects of allergen challenge on large and small airway reactivity in mice. *PLoS One*. 2013;8(9):e74101. doi:10.1371/journal.pone.0074101

25. van den Berge M, Ten Hacken NHT, Cohen J, et al. Small airway disease in asthma and COPD: clinical implications [published correction appears in Chest. 2011 Apr;139(4):972]. *Chest*. 2011;139(2):412–423. doi:10.1378/chest.10-1210

26. Carroll N, Cooke C, James A. The distribution of eosinophils and lymphocytes in the large and small airways of asthmatics. *Eur Respir J*. 1997;10(2):292–300. doi:10.1183/09031936.97.10020292

27. Taha RA, Minshall EM, Miotto D, et al. Eotaxin and monocyte chemotactic protein-4 mRNA expression in small airways of asthmatic and nonasthmatic individuals. *J Allergy Clin Immunol*. 1999;103(3 Pt 1):476–483. doi:10.1016/S0091-6749(99)70474-4

28. Cooper PR, Poll CT, Barnes PJ, Sturton RG. Involvement of IL-13 in tobacco smoke-induced changes in the structure and function of rat intrapulmonary airways. *Am J Respir Cell Mol Biol*. 2010;43(2):220–226. doi:10.1165/rcmb.2009-0117OC

29. Manson ML, Säfholm J, James A, et al. IL-13 and IL-4, but not IL-5 nor IL-17A, induce hyperresponsiveness in isolated human small airways. *J Allergy Clin Immunol*. 2020;145(3):808–817.e2. doi:10.1016/j.jaci.2019.10.037

30. Zhang Y, Li X, He M, et al. The effects of neutralizing anti-murine interleukin-17A monoclonal antibody on ozone-induced inflammation and glucocorticoids insensitivity in a murine model of asthma. *Biomed Pharmacother*. 2019;114:108786. doi:10.1016/j.biopha.2019.108786

31. Bao W, Zhang X, Lv C, et al. The value of fractional exhaled nitric oxide and forced mid-expiratory flow as predictive markers of bronchial hyperresponsiveness in adults with chronic cough. *J Allergy Clin Immunol Pract*. 2018;6(4):1313–1320. doi:10.1016/j.jaip.2017.09.026

32. van der Wiel E, Postma DS, van der Molen T, et al. Effects of small airway dysfunction on the clinical expression of asthma: a focus on asthma symptoms and bronchial hyper-responsiveness. *Allergy*. 2014;69(12):1681–1688. doi:10.1111/all.12510

33. Kang SH, Kim HY, Seo JH, et al. Bronchial hyperresponsiveness to methacholine and AMP in children with atopic asthma. *Allergy Asthma Immunol Res*. 2012;4(6):341–345. doi:10.4168/aair.2012.4.6.341

34. Cohen J, Douma WR, Ten Hacken NH, et al. Ciclesonide improves measures of small airway involvement in asthma. *Eur Respir J*. 2008;31(6):1213–1220. doi:10.1183/09031936.00082407

35. Bonser LR, Erle DJ. Airway mucus and asthma: the role of MUC5AC and MUC5B. *J Clin Med*. 2017;6(12):112. doi:10.3390/jcm6120112

36. Lipworth B, Manoharan A, Anderson W. Unlocking the quiet zone: the small airway asthma phenotype. *Lancet Respir Med*. 2014;2(6):497–506. doi:10.1016/S2213-2600(14)70103-1

37. Tagaya E, Tamaoki J. Mechanisms of airway remodeling in asthma. *Allergol Int*. 2007;56(4):331–340. doi:10.2332/allergolint.R-07-152

38. Halayko AJ, Salari H, Ma X, Stephens NL. Markers of airway smooth muscle cell phenotype. *Am J Physiol*. 1996;270(6 Pt 1):L1040–51. doi:10.1152/ajplung.1996.270.6.L1040

39. Ramos-Barbón D, Fraga-Iriso R, Brienza NS, et al. T Cells localize with proliferating smooth muscle alpha-actin+ cell compartments in asthma. *Am J Respir Crit Care Med*. 2010;182(3):317–324. doi:10.1164/rccm.200905-0745OC

40. Maarsingh H, Bidan CM, Brook BS, et al. Small airway hyperresponsiveness in COPD: relationship between structure and function in lung slices. *Am J Physiol Lung Cell Mol Physiol*. 2019;316(3):L537–L546. doi:10.1152/ajplung.00325.2018

41. Panettieri RA. The Role of Neutrophils in Asthma. *Immunol Allergy Clin North Am*. 2018;38(4):629–638. doi:10.1016/j.iac.2018.06.005